

Supporting Information for
Using Convolutional Neural Networks to Emulate Seasonal Tropical Cyclone Activity

Dan Fu^{1*}, Ping Chang^{1,2}, Xue Liu¹

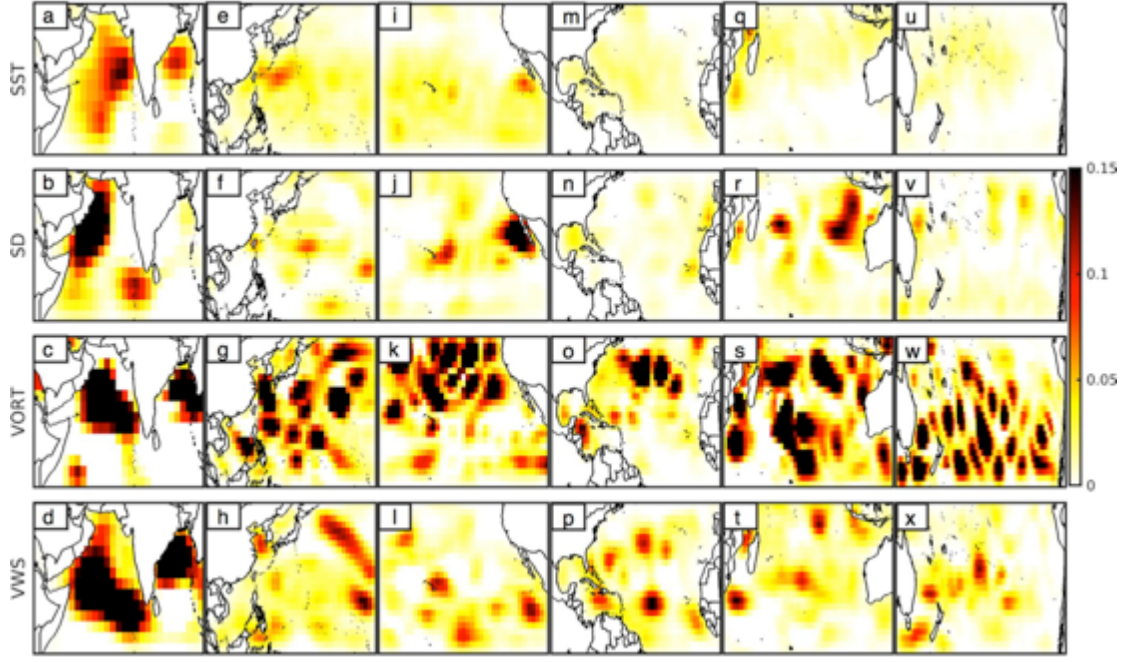
1. Department of Oceanography, Texas A&M University, College Station, TX, USA
2. Department of Atmospheric Sciences, Texas A&M University, College Station, TX, USA

*Corresponding author Email: fudan1991@tamu.edu; ORCID: 0000-0001-6423-6117

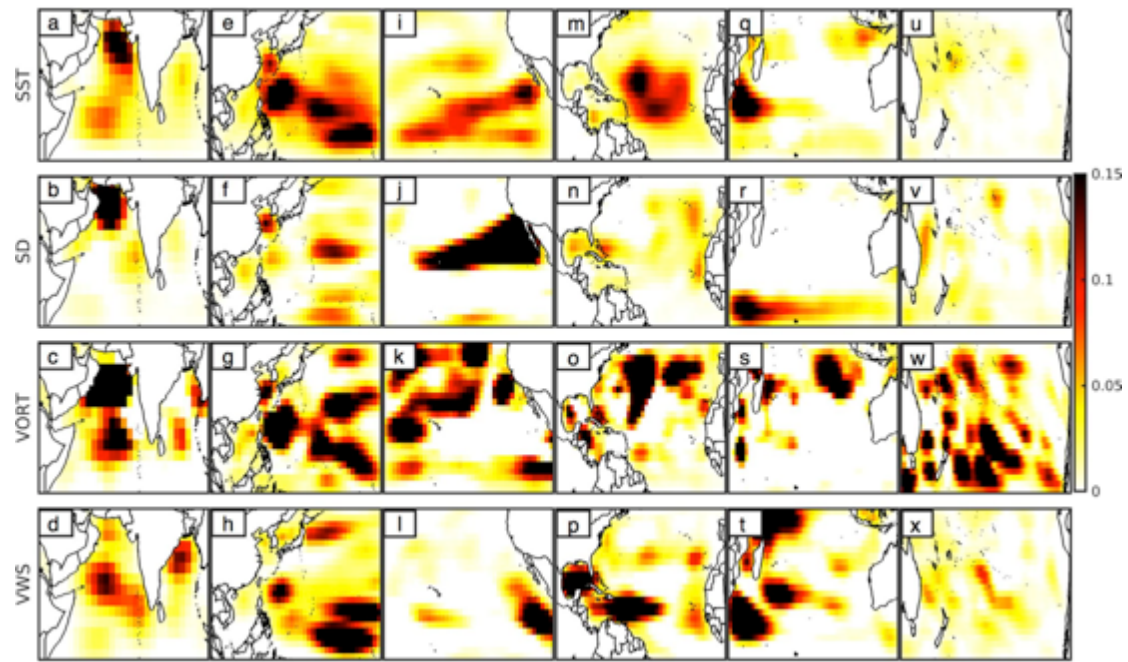
Contents of this file:

Figure S1 to S6

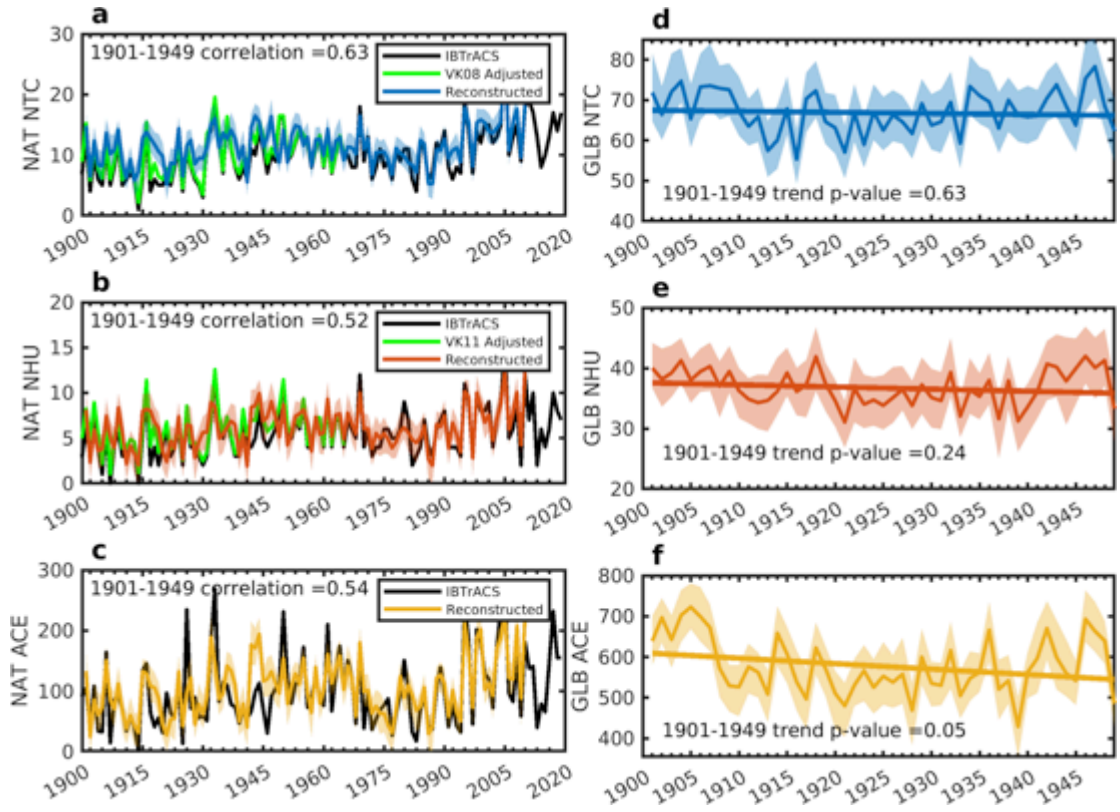
Table S1



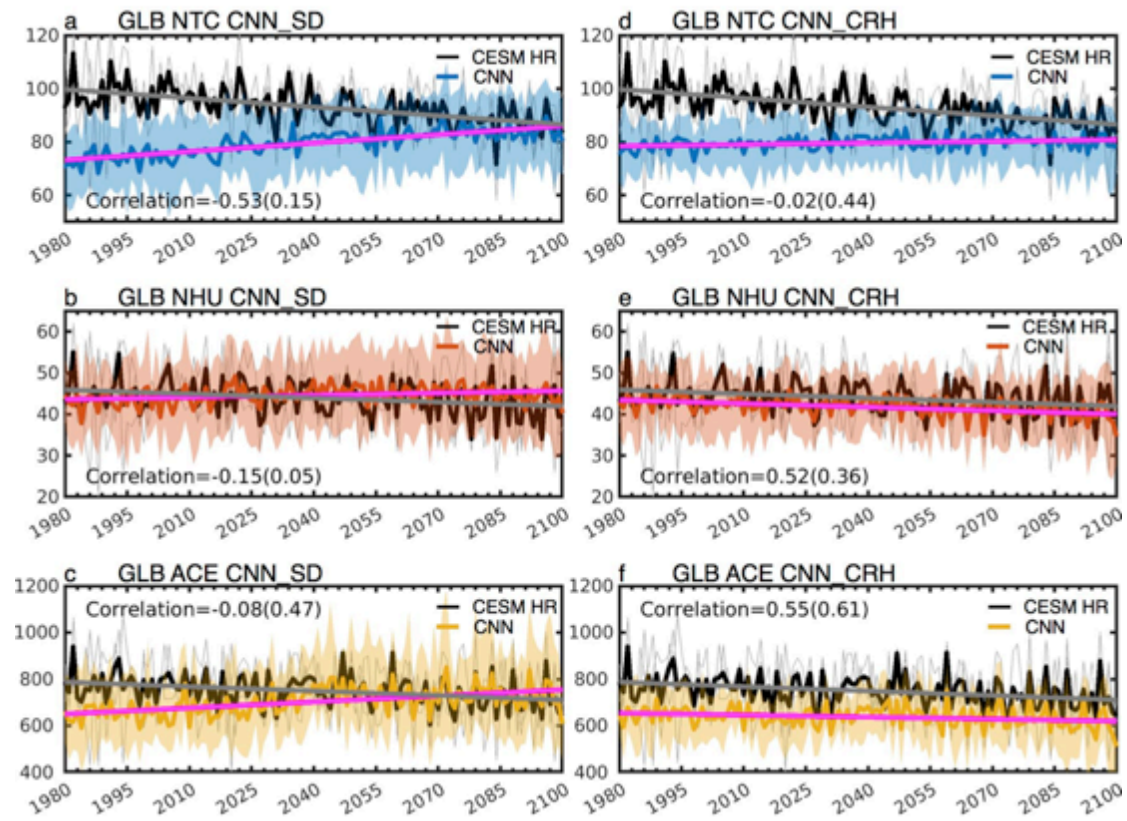
Supplementary Figure 1: Occlusion sensitivity maps that highlight the relative importance and contributions in emulating seasonal NHU in different ocean basins. (a)-(d): Relative importance of SST, saturation deficit (SD), 850hPa vorticity and vertical wind shear in NIO, respectively. (e)-(h), (i)-(l), (m)-(p), (q)-(t), And (u)-(x) are similar, but for the relative importance and contributions of 4 variables in WNP, ENP, NAT, SIO and SPO, respectively. Areas in the map with higher values correspond to regions of input variables that contribute more significantly to impact the CNN accuracy. Intuitively, the sensitivity map shows which area most affect the prediction RMSE when changed. Refer main text for details.



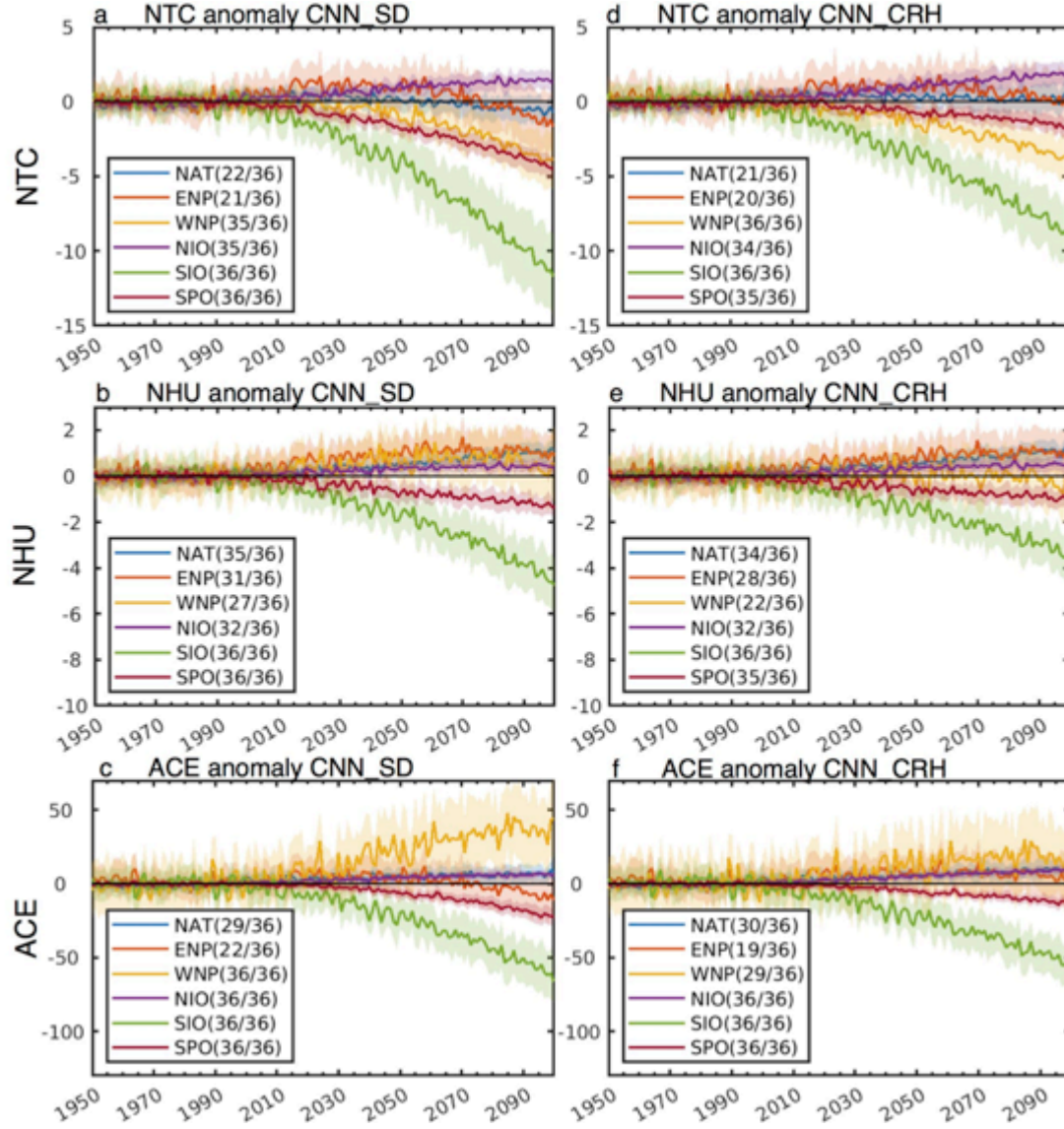
Supplementary Figure 2: Similar as to Supplementary Figure 1, but for occlusion sensitivity maps for ACE.



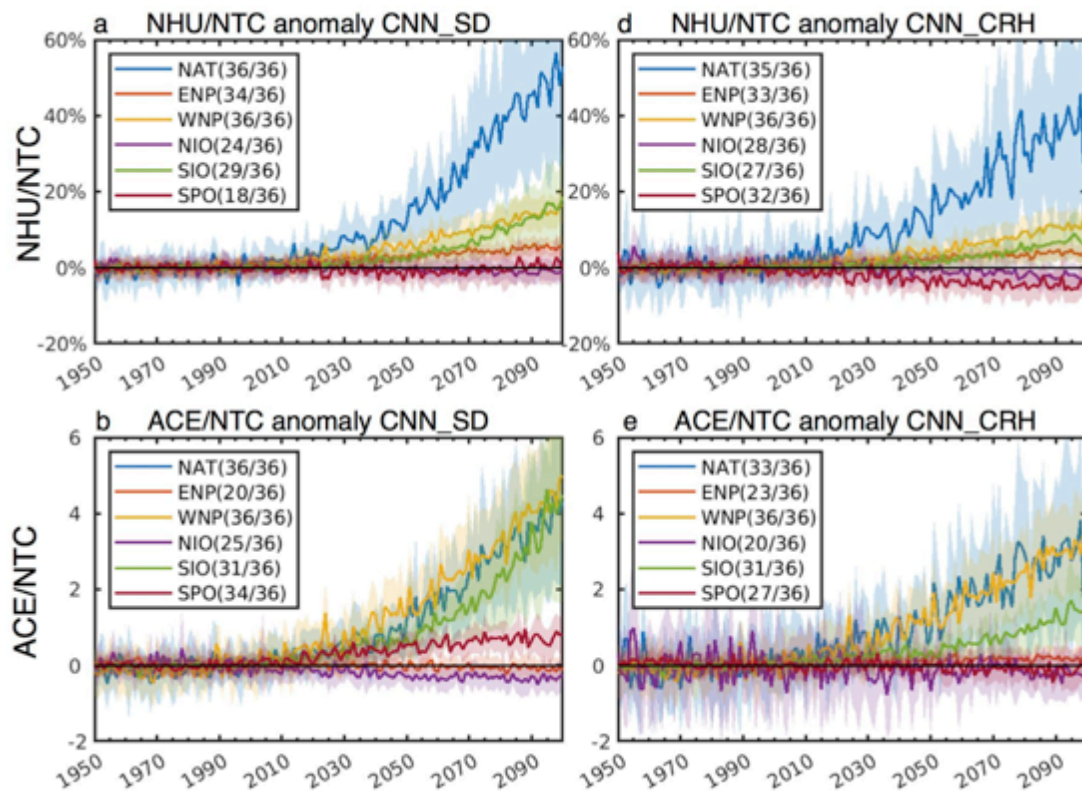
Supplementary Figure 3: Time-series of NAT seasonal mean (a) NTC, (b) NHU, and (c) ACE from the IBTrACS observation in black, adjusted NTC and NHU observation based on Vecchi and Knutson (2008, 2011) in green, and CNN reconstruction based on the ECMWF's Coupled Reanalysis of the Twentieth Century (CERA-20C) for them period 1901-2010. Pearson correlation coefficient between linear-trend removed adjusted observations and CNN reconstructions during 1901-1965 are listed in each panel. Note that, data before 1950 are not used in the CNN training. (d)-(f) Are similar, but for global integration results. We do not show global IBTrACS observation results as other TC active basins outside NAT only provide data since 1949.



Supplementary Figure 4: Time-series of 3-member ensemble mean CESM HR dynamically resolved TC activity (black) and transfer-learned CNN_SD emulated global (a) NTC (blue), (b) NHU (red) and (c) ACE (yellow). Thin grey lines denote CESM HR 3 individual ensemble member, and color shadings indicate ranges across 600-member CNN ensembles. Pearson correlation coefficients between 1980-2100 are listed in each panel. The linear-trend-removed correlation coefficients are listed in the parentheses. Note that, CESM HR data after 1980 are not used in the CNN training. (d)-(f) Are similar, but using the alternative trained CNN model with column relative humidity (CNN_CRH), rather than saturation deficient (CNN_SD), as the CNN predictor variables.



Supplementary Figure 5: Time-series of CNN_SD emulated anomalous (a) NTC, (b) NHU, and (c) ACE in different ocean basins, with the large-scale environmental conditions projected by 36 different CMIP6 model under historical forcing and shared socio-economic pathway 5-8.5 (SSP585). Anomalies are computed as the departures from their 1980-1999 climatology. Standard deviation among 36 CMIP6 models are shown as shadings, while multi-model mean is plotted in lines. The number of individual models with consistent sign of trend as to the multi-model mean is shown in the legend. (e)-(f) Are similar, but for the CNN_CRH emulated CMIP6 projection.



Supplementary Figure 6: Similar to Supplementary Figure 5, but for the ratio of emulated NHU/NTC, and ACE/NTC.

Supplementary Table 1: 36 CMIP6 models utilized for the CNN future projections.

Institution	Model Name
Commonwealth Scientific and Industrial Research Organisation (CSIRO), Australia	ACCESS-CM2
	ACCESS-ESM1-5
The Alfred Wegener Institute, Helmholtz Centre for Polar and Marine Research, Germany	AWI-CM-1-1-MR
Beijing Climate Center, China	BCC-CSM2-MR
Chinese Academy of Meteorological Sciences, China	CAMS-CSM1-0
National Center for Atmospheric Research, United States	CESM2
Euro-Mediterranean Centre on Climate Change	CMCC-CM2-SR5
	CMCC-ESM2
National Center for Meteorological Research, Météo-France and CNRS laboratory, France	CNRM-CM6-1
	CNRM-CM6-1-H
	CNRM-ESM2-1
Canadian Centre for Climate Modelling and Analysis, Canada	CanESM5
	CanESM5-CanOE
Department of Energy, United States	E3SM-1-1
European Earth System Model, EU	EC-Earth3
Chinese Academy of Sciences, China	FGOALS-f3-L
First Institute of Oceanography, China	FIO-ESM-2-0
U.S. Department of Commerce/National Oceanic and Atmospheric Administration (NOAA)/Geophysical Fluid Dynamics Laboratory (GFDL), USA	GFDL-CM4
	GFDL-ESM4
National Aeronautics and Space Administration (NASA)/Goddard Institute for Space Studies (GISS), United States	GISS-E2-1-G
Met Office Hadley Centre, United Kingdom	HadGEM3-GC31-LL
	HadGEM3-GC31-MM
Indian Institute of Tropical Meteorology, India	IITM-ESM
Institute for Numerical Mathematics, Russia	INM-CM4-8
	INM-CM5-0
Institut Pierre-Simon Laplace, France	IPSL-CM6A-LR
Korea Meteorological Administration, Korea	KACE-1-0-G
Korea Institute of Ocean Science & Technology, Korea	KIOST-ESM
University of Arizona, United States	MCM-UA-1-0
Center for Climate System Research (University of Tokyo), National Institute for Environmental Studies, and Frontier Research Center for Global Change (JAMSTEC), Japan	MIROC-ES2L
	MIROC6
Max Planck Institute for Meteorology, Germany	MPI-ESM1-2-LR
Meteorological Research Institute, Japan	MRI-ESM2-0
Nanjing University of Information Science and Technology, China	NESM3
Norwegian Meteorological Institute, Norway	NorESM2-MM
Met Office Hadley Centre, United Kingdom	UKESM1-0-LL